

## PREDICTION OF FORMED PHASES IN TWO HIGH ENTROPY SYSTEMS

MAZANCOVÁ Eva<sup>1</sup>, SAKSL Karel<sup>2</sup>, KUČERA Pavel<sup>1</sup>

<sup>1</sup> VSB - Technical University of Ostrava, Faculty of Metallurgy and Materials Engineering, Ostrava, Czech Republic, EU, [eva.mazancova@vsb.cz](mailto:eva.mazancova@vsb.cz), [paul.kucera@seznam.cz](mailto:paul.kucera@seznam.cz)

<sup>2</sup> Institute of Material Research of SAS, Košice, Slovakia, EU, [ksaksl@imr.saske.sk](mailto:ksaksl@imr.saske.sk)

### Abstract

Work deals with phase formation of eight high entropy alloys of  $\text{FeCu}_x\text{Cr}_{1-x}\text{MnNi}$  type and of three alloys of  $\text{Fe}_x\text{CuCrMnNi}$  system with high entropy effect. Predicted compositions of phases using Ni and Cr equivalents and by use of valence electron concentration are compared with real finding of presented phases in all aforesaid systems. Types of phases were detected by hard X-ray synchrotron micro-diffraction. With increasing Cr content in  $\text{FeCu}_x\text{Cr}_{1-x}\text{MnNi}$  system double FCC phases changed into double FCC with BCC phases under simultaneously increase of yield stress. In  $\text{Fe}_x\text{CuCrMnNi}$  system with atypical higher Fe content double FCC phases were detected with their different volume fractions. With increasing Fe content as a BCC stabilizer a rise of yield stress was detected. In both investigated systems, predicted results of formed phases partially differed from founded phases using synchrotron.

**Keywords:**  $\text{FeCu}_x\text{Cr}_{1-x}\text{MnNi}$  high entropy system,  $\text{Fe}_x\text{CuCrMnNi}$  high entropy system, Ni - Cr equivalents, valence electron concentration, phases composition

### 1. INTRODUCTION

High entropy alloys (HEAs) are formed by five metallic elements minimally and represent a novel alloy design concept. By now investigated HEAs had showed unique mechanical properties [1-3], favourable electric and magnetic characteristics [2, 3], wear resistance [4] and corrosive properties [5-7]. HEAs are suitable both for cryogenic conditions and for creep applications [3, 8]. Outstanding HEAs properties can be reached thanks a) high entropy effect, b) sluggish diffusion, c) possibility of crystallographic lattice torsion and d) HEAs position in Ashby's diagram [9, 10]. In HEAs, there are only solid solutions possible. The most frequently are FCC, BCC and/or their mixture. The FCC stabilizers are Ni, Co, Mn, Cu, C, N etc. and Cr, Fe, Mo, Si, Nb etc. are effective as the BCC stabilizers. According number of elements, their volume fraction and type, resp. their atomic radius, and thanks the sluggish diffusion during extremely high cooling rate at manufacturing process and mentioned crystallographic lattice torsion, resp. due to the atomic-level strain energy [3] different types of phases can be formed. A higher portion of one element can change e.g. FCC structure into mixture of FCC and BCC and/or into BCC with quite different properties. To predict the changes in microstructure in HEAs, resp. to estimate type of phases, Ni and Cr equivalents ( $\text{Ni}_{\text{eq}}$  and  $\text{Cr}_{\text{eq}}$ ) are often used, similar like in stainless steels [11]. The higher the  $\text{Ni}_{\text{eq}}$ , the easier it is to obtain FCC structure. Conversely, the higher the  $\text{Cr}_{\text{eq}}$ , the easier it is to form BCC structure. Ren et al [11] effectively modified aforesaid equivalents. Guo et al. [12] suggested using the valence electron concentration (VEC) to predict the FCC and BCC solid solution structures of HEAs. He worked with  $\text{Al}_x\text{Cr}_y\text{Cu}_z\text{FeNi}_2$  alloys and summarized the relationship between VEC and structure as follows: for FCC, VEC is higher than 8, for BCC the VEC is lower than 6.8 and between the both boundaries mixture of FCC and BCC should be detected.

Presented work is aimed at prediction of phase type formed after casting in  $\text{FeCr}_{1-x}\text{Cu}_x\text{MnNi}$  HEAs and especially in atypical  $\text{Fe}_x\text{CrCuMnNi}$  alloy types with higher Fe contents representing cheaper variants of materials with high entropy effect. Results are compared with really found phase types using a hard synchrotron X-ray diffraction.

**Table 1** Investigated alloys with high entropy effect and detected phases using XDR

	<b>A</b> FeCu <sub>1.75</sub> Cr <sub>0.25</sub> MnNi	<b>B</b> FeCu <sub>1.5</sub> Cr <sub>0.5</sub> MnNi	<b>C</b> FeCu <sub>1.25</sub> Cr <sub>0.75</sub> MnNi	<b>D</b> FeCuCrMnNi
phase	FCC <sub>1</sub> +FCC <sub>2</sub>	FCC <sub>1</sub> +FCC <sub>2</sub>	FCC <sub>1</sub> +FCC <sub>2</sub> +BCC	FCC <sub>1</sub> +FCC <sub>2</sub> +BCC
alloy	<b>E</b> FeCu <sub>0.75</sub> Cr <sub>1.25</sub> MnNi	<b>F</b> FeCu <sub>0.5</sub> Cr <sub>1.5</sub> MnNi	<b>G</b> FeCu <sub>0.25</sub> Cr <sub>1.75</sub> MnNi	<b>H</b> FeCuCr <sub>2</sub> MnNi
phase	FCC <sub>1</sub> +FCC <sub>2</sub> +BCC	FCC <sub>1</sub> +FCC <sub>2</sub> +BCC	FCC <sub>1</sub> +FCC <sub>2</sub> +BCC	FCC+BCC
alloy	<b>CH</b> Fe <sub>2.5</sub> CuCrMnNi	<b>I</b> Fe <sub>3</sub> CuCrMnNi	<b>J</b> Fe <sub>3.5</sub> CuCrMnNi	
phase	FCC <sub>1</sub> +FCC <sub>2</sub>	FCC <sub>1</sub> +FCC <sub>2</sub>	FCC <sub>1</sub> +FCC <sub>2</sub>	

## 2. EXPERIMENTAL

For evaluation eight HEAs of FeCu<sub>x</sub>Cr<sub>1-x</sub>MnNi type (named **A** up to **H**) were used which were laboratory manufactured and analyzed using hard X-ray micro-diffraction (XRD) as was presented in work [13] and three alloys with high entropy effect of Fe<sub>x</sub>CuCrMnNi type (named **CH**, **I**, **J**) which are summarized in **Table 1** with analyzed phases types. All HEAs were synthesized by vacuum arc-melting method in Compact Arc Melter MAM-1 (**Figure 2** left). Preparation of ingots was carried out in argon at temperature up to 3 500 °C and followed by suction casting of a melt to cooled Cu mould. Samples in form of ingots of 3 mm diameter and 35 mm in length were made. During all process, vacuum was necessary to generate several times by assisted rotary pump (at 5.10<sup>-2</sup> mbar). For the production of any ingot, not only critical parameter of vacuum level is important, but in particular the temperature of the melting, at which the melt is cast. Standard weight was approximately 2 - 3 g. Further, ingots were cut to rolls with dimensions of 6 (length) x 3 mm. Manufactured samples were put to tensile test. Tensile tests for two samples of each alloy (200 KN Zwick-Extensometer) at ambient temperature (in the beginning testing rate corresponded to 0.083 mm / s, from R(v) 0.017 mm / s), micro-hardness HV0.5 (LECO 2000) over each sample in transverse section. To determine phase composition and microstructure parameters of studied alloys a hard X-ray diffraction experiment was performed at beamline P07 at PETRA III (electron storage ring operating at energy of 6 GeV with beam current of 100 mA). During the experiment, monochromatic synchrotron radiation of energy 99.5 keV ( $\lambda = 0.012587$  nm) was used. Measurements were carried out in transmission mode, when the samples were illuminated for 7.5 s by well collimated incident beam of 0.5 mm x 0.5 mm cross-section and the XRD patterns were recorded using a 2D detector (Perkin Elmer 1621). The collected 2D XRD data were then integrated into 2 Theta space by use of Fit2D software [14]. Sample detector distance, detector orthogonality with respect to the incoming radiation as well as precise radiation energy was determined by fitting a standard reference LaB<sub>6</sub> (NIST SRM 660a) sample. Other information concerning synchrotron application is accessible in paper [14]. Results from synchrotron were compared with predicted data found using Ni equivalent (Ni<sub>eq</sub>), Cr equivalent (Cr<sub>eq</sub>) presented in modified form in works [3, 11] and valence electron concentration (VEC) according Guo's concept [10].

## 3. RESULTS AND THEIR ANALYSIS

Records (XRD patterns) of presented phases in FeCu<sub>1-x</sub>Cr<sub>x</sub>MnNi HEA (named **A** up to **H**) were former reported in paper [13] and are shortly summarized in **Table 1** and **Figure 1**. Detected phases using synchrotron radiation in the investigated Fe<sub>x</sub>CuCrMnNi system (alloys named **CH**, **I**, **J**) complete above mentioned table and separately can be seen in **Figures 2, 3**. With exception of HEAs **A** and **B**, which are on the base of double FCC, phase all other alloys showed mixture phases of FCC<sub>1</sub>, FCC<sub>2</sub> and BCC type (alloy **C** up to **G**), resp. one FCC with BCC (alloy **H**).

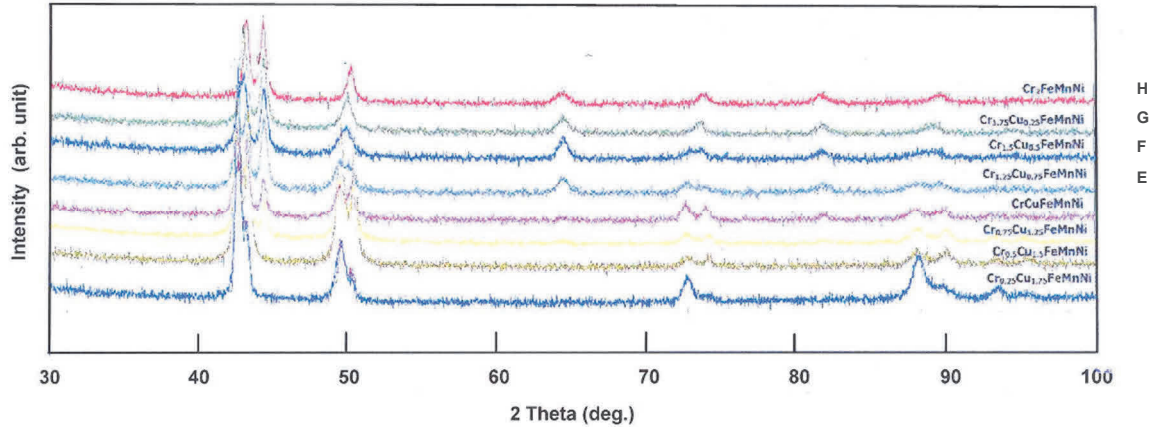


**Figure 1** XRD patterns of FeCu<sub>1-x</sub>Cr<sub>x</sub>MnNi (named **A** up to **H**)

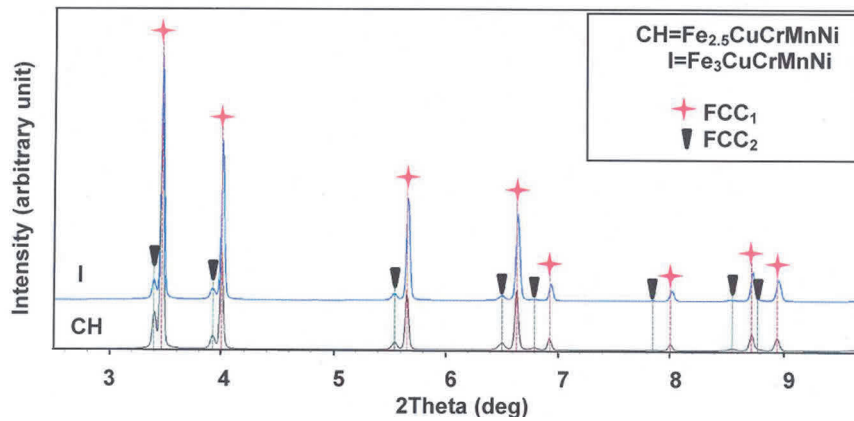


**Figure 2** XRD patterns of Fe<sub>2.5</sub>CuCrMnNi (**CH**) and Fe<sub>3</sub>CuCrMnNi (**I**) steels

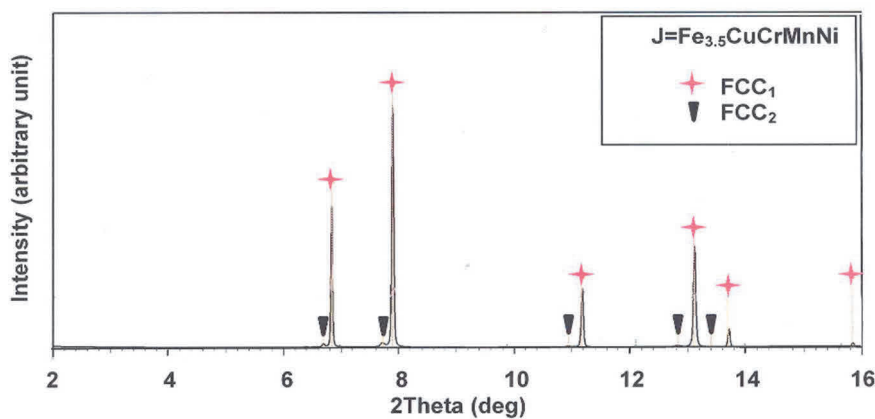


**Figure 3** XRD pattern of Fe<sub>3.5</sub>CuCrMnNi (**J**) steels

With increasing Cr content to the exclusion of Cu portion BCC phase was increasing being in accord with Cr stabilizer [3]. In Fe<sub>2.5</sub>CrCuMnNi alloy major FCC<sub>1</sub> phase had lattice parameter  $a = 0.3606$  nm, while in the second minor FCC<sub>2</sub> it was  $0.3677$  nm. Volume fractions of the FCC<sub>1</sub> and FCC<sub>2</sub> phases occupied approximately 83 % and 17 %, respectively (percentages determined by the Rietveld refinement method [14]). In the Fe<sub>3</sub>CrCuMnNi lattice parameter of the FCC<sub>1</sub> phase corresponded to  $0.36$  nm (94 vol. %) and of the other minor FCC<sub>2</sub> phase to  $0.3679$  nm (6 vol. %), while in Fe<sub>3.5</sub>CuCrMnNi dominating phase FCC<sub>1</sub> represented 96 vol. %

with lattice parameter  $a = 0.36$  nm, minority phase FCC<sub>2</sub> was detected in 4 % and lattice parameter  $a = 0.3677$  nm. With increasing Fe content FCC<sub>1</sub> phase portion was going up to the exclusion of FCC<sub>2</sub> phase. With changes of FCC phase portions and/or formation of the BCC structure, differences in their basic mechanical properties are obvious. With increasing Cr portion to the exclusion of Cu in FeCu<sub>1-x</sub>Cr<sub>x</sub>MnNi system, yield stress (YS) in pressure shows increasing tendency as it from **Figure 4** follows. Practically none differences between samples tested at ambient and cryogenic temperature were observed. In Fe<sub>x</sub>CrCuMnNi system increasing Fe content shows similar trend as it from **Figure 5** follows, even when YS was tested in tensile.

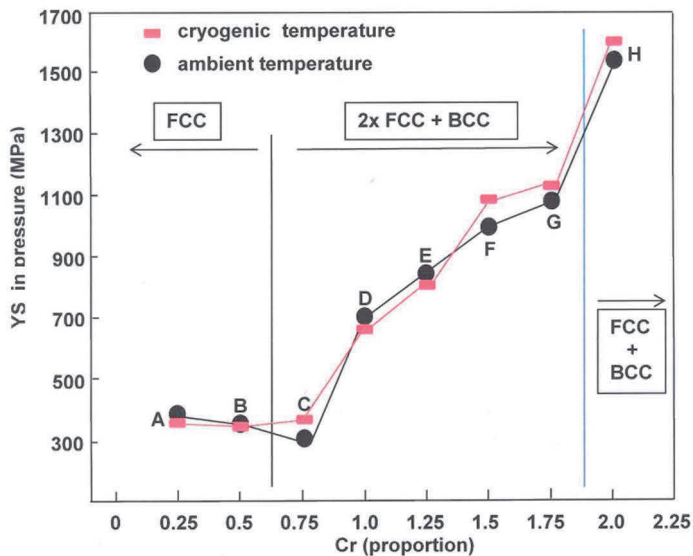


**Figure 4** Changes of yield stress (YS), resp. phases in dependence on Cr content

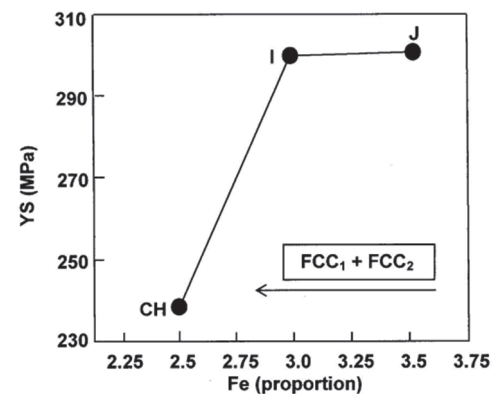


**Figure 5** Changes of yield stress (YS), resp. phases in dependence on Fe content

When in the HEAs is a higher portion of BCC stabilizers and elements showing greater atomic radius the more torsion and stress of lattices can be awaited, later leading to change of structure composition and increase of strength [3]. Transitions from FCC structure into mixture FCC with BCC and/or to BCC are associated with steep strength increase as it was demonstrated e.g. by Yeh et al and Kao et al [4, 15]. In FeCu<sub>x</sub>Cr<sub>1-x</sub>MnNi HEAs BCC structure appeared when Cr content amounted to 15 at. %. In case the Cr content was on the level of 35 at. % increase of yield stress by 758 MPa (at ambient temperature) and/or by 725 MPa (at cryogenic temperature) was registered, representing 245 % and/or 183 % growth. Phase composition of FeCuCr<sub>2</sub>MnNi HEA (showing 40 at. % of Cr - alloy **H**) resulted in one FCC and BCC phases. The other 5 at. % increase of Cr in given HEA in comparison with the HEA **G** represented further growth of yield stress approximately by 43 %, resp. 42 % for cryogenic temperature. On the contrary, according Ostroushko et al [13], double portion of Cu (Cu amounted to 40 at. %) FeCu<sub>2</sub>CrMnNi resulted in double FCC phases only, because FCC stabilizers were in majority. In the other investigated system, between alloys **CH** and **I** (by 4.4 at. % higher Fe content) was recorded 26 % increase in yield stress. In alloy **J** higher Fe portion by 8.2 at. % resulted in 0.5 % (insignificant) yield stress increase. Results of prediction of formed phases in alloys showing high entropy effect using  $Ni_{eq}$  and  $Cr_{eq}$  [3, 11] and by use of VEC according to concepts described in works [3, 10] are summarized in **Figures 6, 7**. Results of the first way of phase determination named **A** and **B** showed double FCC structure only, while the rest of nine alloys named **C, D, E, F, G, H** and **CH, I, J** were associated with FCC and BCC in different portions. In case of the second way (VEC) of phase prediction not only alloys **A** and **B**, however **C, D, CH, I** and **J** should be formed by double FCC and/or by one FCC (case of **H** HEA) only. In comparison with results from synchrotron the founded disproportions are distinguished by red colour in proper points as it can be seen from **Figures 6** and **7**. According to VEC alloys **C** and **D** are lying close the transition boundary FCC / mixed FCC + BCC and represent typical HEAs unlike the alloys **CH, I, J** having atypical higher Fe contents and in

spite of it show high entropy effect. Presented iron represents the largest disparity between HEA and FCC-Fe migration activation energy and it could be one of the reason of observed differences between predicted and real results.

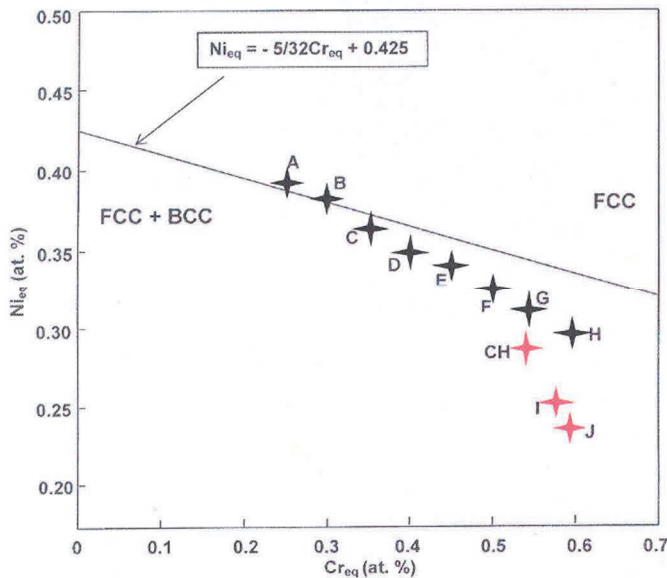


**Figure 6** Predicted phases in investigated two systems by use of  $Ni_{eq}$  and  $Cr_{eq}$

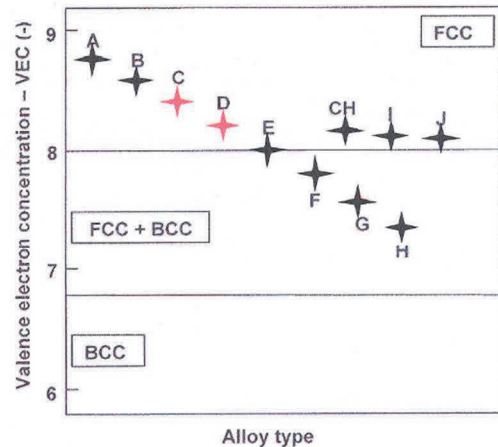


**Figure 7** Predicted phases in investigated two systems by use of VEC

Regarding comparison of predicted phases and those really detected, Yeh et al [8] and Guo et al [10] have admitted overlapping of predicted regions and revealed reality. Discrepancies in some properties of HEAs were also detected by Tsai et al [16] and Middleburgh [17] who ascribed these findings to sluggish diffusion in HEAs, lower lattice potential energy, to a combination of effect including magnetic properties, frustrated lattice and consequence of the change in Fe behaviour from low temperature ferrite to high temperature austenite. Generally, Fe shows the largest disparity between HEA and FCC-Fe migration activation energy.

#### 4. CONCLUSION

Work deals with prediction of eight high entropy alloys of  $FeCu_xCr_{1-x}MnNi$  type and of three alloys of  $Fe_xCuCrMnNi$  system showing high entropy effect. From hard X-ray diffraction experiment performed using synchrotron HEAs of the first mentioned type with maximal 10 at. % of Cr showed double FCC phases, while HEAs with increasing Cr contents were formed beside double FCC phases and/or one FCC phase (in case of  $FeCuCr_2MnNi$ ) by BCC phase. All alloys of the  $Fe_xCuCrMnNi$  type (38.5, 42.9 and 46.7 at. % of Fe) revealed double FCC phases. Predicted phases types using Ni and Cr equivalents showed conformity with reality for all HEAs of  $FeCu_xCr_{1-x}MnNi$  type, while for all investigated set of  $Fe_xCuCrMnNi$  alloys discrepancies were detected. By use of valence electron concentration (VEC) predicted phases of these  $Fe_xCuCrMnNi$  alloys corresponded to reality unlike alloys of  $FeCu_{1.25}Cr_{0.75}MnNi$  and  $FeCuCrMnNi$  type which should be formed according to VEC by FCC phase only. In case of the first system type the disproportions appeared just on the transition of the FCC into FCC and BCC and so the mathematical approach could not be quite perfect. Regarding the  $Fe_xCuCrMnNi$  alloys, those showed higher Fe contents than is current for HEAs. Iron represents the largest disparity between HEA and FCC-Fe migration activation energy and it could be main reason of observed differences between predicted and real results.

## ACKNOWLEDGEMENTS

*This paper was created within the project No. LO1203 "Regional Materials Science and Technology Centre - Feasibility program" funded by Ministry of Education, Youth and Sports of Czech Republic. K. Saksl is grateful to the scientific Grant Agency of the ministry of education, Science, research and Sport of the Slovak Republic and the Slovak Academy of Science (VEGA project No. 2/0021/16).*

## REFERENCES

- [1] RAZUAN, R., JANI, N.A., HURAN, M.K., TALARI, M.K. Microstructure and hardness properties investigation of Ti and Nb added FeNiAlCuCrTi<sub>x</sub>Nb<sub>y</sub> high entropy alloys. *Trans. Indian Inst. Met.*, 2013, vol. 66, pp. 309-312.
- [2] MURTY, B.S., YEH, J.W., RANGANATHAN, S. *High entropy alloys*. 1<sup>st</sup> ed. London: Butterworth-Heinemann, 2014, 204 p.
- [3] ZHANG, Y., ZHUO, T.T., TANG, T., GAO, M.C., DAHMEN, K.A., LIAW, P.K., LU, Z.P. Microstructures and properties of high-entropy alloys. *Prog. Mater. Sci.*, 2014, vol. 61, pp. 1-93.
- [4] YEH, J.W., CHEN, S.K., LIN, S.J., GAN, J.Y., CHIN, T.S., SHUN, T.T., TSAU, C.H., CHANG, S.Y. Nanostructured high-entropy alloys with multiple principal elements: novel alloy design concepts and outcomes. *Adv. Eng. Mater.*, 2004, vol. 6, no. 5, pp. 299-303.
- [5] CHEN, Y.Y., DUVAL, T., HUNG, U.D., YEH, J.W., SHIH, H.C. Microstructure and electrochemical properties of high entropy alloys-a comparison with type-304stainless steel. *Corros. Sci.*, 2005, vol. 47, no. 9, 2257-79.
- [6] DUFALOVÁ, Z., MAZANCOVÁ, E., SAKSL, K., OSTROUSHKO, D., ĎURIŠIN, M., BALGA, D., SZABO, J., KUČERA, P. Selected properties of two high entropy alloys. In *METAL 2016: 25rd International Conference on Metallurgy and Materials*. Ostrava: TANGER, 2016, pp. 700-705.
- [7] CHOU, Y.L., YRH, J.W., SHIN, H.C. The effect of molybdenum on the corrosion behaviour of the high-entropy alloys Co<sub>1.5</sub>CeFeNi<sub>1.5</sub>Ti<sub>0.5</sub>Mo<sub>x</sub>. *Corros. Sci.*, 2010, vol. 52, pp. 2571-2581.
- [8] YEH, J.W. Recent progress in high-entropy alloys. *Ann. Chim. Sci. Mater.*, 2006, vol. 31, pp. 633-648.
- [9] GLUDOVATZ, B., HOHENWARTER, A., CATOOR, D., CHANG, E.H., GEORGE, E.P., RITCHIE, R.O. A fracture resistant of high-entropy alloy for cryogenic applications. *Sci.*, 2014, vol. 345, pp. 1153-1158.
- [10] GUO, S., HU, Q., NG, C., Liu, C.T. More than entropy in high-entropy alloys: forming solid solutions or amorphous phase. *Intermet.* 2013, vol. 41, pp. 96-103.
- [11] REN, B., LIU, Z.X., LI, D.M., SHI, L., CAI, B., WANG, M.X. Effect of elemental interaction on microstructure of CuCrFeNiMn high entropy alloy system. *J. Alloys Comp.*, 2010, vol. 493, pp. 148-153.
- [12] GUO, S., NG, C., LU, J., LIU, C.T. Effect of valence electron concentration on stability of fcc or bcc phase in high entropy alloys. *J. Appl. Phys.*, 2011, vol. 109, pp. 103505.
- [13] OSTROUSHKO, D., SAKSL, K., BALGA, D., SZABO, J., ĎURIŠIN, M., MILKOVIČ, O., ZUBKO, P. Microstructures and base mechanical properties of Cr<sub>1-x</sub>Cu<sub>x</sub>MnFeNi high entropy alloys. In *METAL 2015: 24rd International Conference on Metallurgy and Materials*. Ostrava: TANGER, 2015, pp. 523-528.
- [14] SAKSL, K., OSTROUSHKO, D., MAZANCOVÁ, E., SZULC, Z., MILKOVIČ, O., ĎURIŠIN, M., BALGA, D., ĎURIŠIN, J., RÚTT, U., GUTTOWSKI, O. Local structure of explosive welded titanium-stainless bimetal. *Int. J. Mater. Res.*, 2015, vol. 106, no. 6, pp. 621-627.
- [15] KAO, Y.F., CHEN, T.J., CHEN, S.K., YEH, J.W. Microstructure and mechanical property of As-cast, homogenized, and deformed Al<sub>x</sub>CoCrFeNi (0≤x≤2) high entropy alloys. *J. Alloy. Comp.*, 2009, vol. 488, pp. 57-64.
- [16] TSAI, M.H., YEH, J.W. High-entropy alloys: A critical review. *Mater. Res. Lett.*, 2014, vol. 2, no. 3, pp. 107-123.
- [17] MIDDLEBURGH, S.C., KING, D.M., LUMPKIN, G.M., CORTIE, M., EDWARDS, L. Segregation and migration of species in the CrCoFeNi high entropy alloy. *J. Alloys Comp.*, 2014, vol. 599, pp. 179-182.